Chapter 3

Chapter 3

Mouse models for Xeroderma pigmentosum group A and group C show divergent cancer phenotypes

Melis JPM, Wijnhoven SW, Beems RB, Roodbergen M, van den Berg J, Moon H, Friedberg E, van der Horst GTJ, Hoeijmakers JHJ, Vijg J, van Steeg H.

Mouse models for Xeroderma pigmentosum group A and group C show divergent cancer phenotypes

Cancer Res. **2008** Mar 1;68(5):1347-53.

"I'll need some information first, just the basic facts"

Comfortably Numb – Pink Floyd, 1979

Abstract

The accumulation of DNA damage is a slow but hazardous phenomenon that may lead to cell death, accelerated aging and cancer. One of the most versatile defense mechanisms against the accumulation of DNA damage is nucleotide excision repair, in which, amongst others, the XPC and XPA protein are involved.

To elucidate differences in the functions of these two proteins comprehensive survival studies with *Xpa*$^{-/-}$, *Xpc*$^{-/-}$ and wild type control, female mice in a pure C57BL/6J background were performed. The median survival of *Xpc*$^{-/-}$ mice showed a significant decrease in survival, while the median survival of *Xpa*$^{-/-}$ mice did not. Strikingly, *Xpa*$^{-/-}$ and *Xpc*$^{-/-}$ mice also showed a phenotypical difference in terms of tumor spectrum. *Xpc*$^{-/-}$ mice displayed a significant increase in lung tumors and a trend towards increased liver tumors compared to *Xpa*-deficient or wild type mice. *Xpa*$^{-/-}$ mice showed a significant elevation in liver tumors. Additionally, *Xpc*-deficient mice exhibited a strong increase in mutant frequency in lung compared to *Xpa*$^{-/-}$ mice, whereas in both models mutant frequency is increased in liver. Our *in vitro* data displayed an elevated sensitivity to oxygen in *Xpc*$^{-/-}$ in mouse embryonic fibroblasts, when compared to *Xpa*$^{-/-}$ and wild type fibroblasts.

We believe that XPC plays a role in the removal of oxidative DNA damage and that therefore *Xpc*$^{-/-}$ mice display a significant increase in lung tumors, a significant elevation in mutant frequency in lung and *Xpc*-deficient embryonic fibroblasts are more sensitive to oxygen when compared to *Xpa*$^{-/-}$ and wild type mice.

Introduction

Cancer remains one of the main causes of death nowadays in both men and women and is accompanied by a kaleidoscope of unsolved questions about the induction and progress of this disease. An important factor in the development of cancer is the accumulation of somatic DNA damage [1]. Normally, several sophisticated defense mechanisms are active to repair the modified DNA to prevent mutations and damage accumulation. Base excision repair (BER) for example will remove most small base modifications (e.g. oxidative DNA damage). Nucleotide excision repair (NER) has a very broad lesion spectrum and is responsible for the removal of bulky, DNA helix-distorting adducts [2-7].

The autosomal recessive disorder Xeroderma pigmentosum (XP) is an elucidative example of the influence of a DNA repair defect on cancer predisposition. XP patients exhibit extreme UV-sensitivity and are predisposed to skin cancer by a 1000-fold higher risk [8;9]. Until now seven complementation groups (XP-A through XP-G) plus a variant form (XP-V) were identified. XP disorders arise from a deficiency in one or more of these XP proteins, which belong to the NER pathway, with the notable exception of the XPV protein, which is involved in translesion synthesis of UV-damaged DNA [10].

NER can be subdivided in two subpathways: global genome NER (GG-NER), which covers the complete genome, and transcription coupled NER (TC-NER), which focuses on repair of the transcribed strand of active genes [11;12]. XPC is associated with the GG-NER while XPA plays a role in both GG-NER and TC-NER. The XPC protein, in complex with the HR23B protein, is responsible for DNA damage recognition [6;13]. Following detection of distorted helix structures, the XPC/HR23B-complex will initiate the GG-NER process [14]. Subsequently, the XPC/HR23B-complex will dissociate from the damaged DNA strand when the transcription factor TFIIH in combination with the XPA and RPA protein set the verification of the DNA damage in motion [15]. XPC-HR23B is dispensable for TC-NER; the CSA and CSB proteins, together with RNA polymerase II stalled at a lesion, fulfill the role of recognition factor in this pathway. As in GG-NER, DNA damage verification in TC-NER requires presence of the TFIIH-XPA-RPA complex [16].

When TC-NER components or the more common elements in NER (e.g. XPA) are affected, very complex clinical features are observed [17]. Patients with a defect in genes unique to GG-NER (like XPC) exhibit fewer clinical symptoms besides cancer. In general, deficiencies in the TC-NER pathway are related to neurodegenerative disorders, while defects in the GG-NER pathway are designated as more cancer prone [18-21].

The XP-C is the most common type of the XP disease in North-America and Europe [22]. This form is only defective in the GG-NER pathway. XP-A patients are disrupted in both their GG-NER and TC-NER pathways. Mutant frequency analyses at the *Hprt* locus in mouse models of these two forms of XP previously uncovered striking differences. *Hprt* mutant frequencies in the spleen of *Xpc*$^{-/-}$ mice in a mixed genetic background were highly elevated in comparison to their wild type controls but also compared to *Xpa*$^{-/-}$, both in a pure C57BL/6J background [23]. This indicates that knockout mouse models of *Xpc* and *Xpa* may also exhibit different spontaneous phenotypes. *Xpc*$^{-/-}$ mice of a mixed background (25% 129, 75% C57BL/6J) were shown to exhibit a high prevalence of lung tumors [24], but this has not been studied in a pure C57BL/6J background. Also a clean comparison with *Xpa*$^{-/-}$ mice has not yet been made.

To refine and expand our knowledge on human XP-A and XP-C, *Xpa*$^{-/-}$ and *Xpc*$^{-/-}$ mice were used. To investigate the phenotypic differences between these mice we performed a more comprehensive study with both mouse models in a pure C57BL/6J background. We compared the lifespan of the two models and determined pathology with the focus on tumor development. In addition, to help explain the differences in tumor outcomes we performed mutation analyses in several organs. Our data suggest that *Xpc*-deficient mice are more sensitive to (oxidative) DNA-damaging agents in the lung compared to the *Xpa*-deficient mice and wild type controls. These findings support evidence provided in various studies that XPC, in addition to its function in GG-NER, is also involved in the repair of oxidative DNA damage. Therefore, *Xpc*$^{-/-}$ mice seem more sensitive to oxidative stress and lung tumor development than their NER-deficient counterparts, *Xpa*$^{-/-}$ mice.

Materials and Methods

Mice

The generation and characterization of *Xpa*$^{-/-}$ and *Xpc*$^{-/-}$ mice and has been described before [25;26]. To obtain a genetically homogenous background, *Xpa*- and *Xpc*-deficient mice were back-crossed over 10 times with C57BL/6J animals (Harlan). To offer the future possibility to monitor genomic instability, the heterozygous mutant mice strains as well as C57BL/6J controls were crossed with pUR288-*lacZ* C57BL/6J transgenic mice line 30, homozygous for *lacZ* integration on chromosome 11 [27]. In the second round of breeding, double heterozygous mice were intercrossed to obtain homozygous mice carrying one locus of the integrated copies of the *lacZ* marker, used in the third breeding round to generate the experimental animals for the aging and cross-sectional studies as described below. Mice were genotyped by a standard PCR reaction using DNA isolated from tail tips. Primers to amplify the wild type and targeted *Xpa* and *Xpc* allele, as well as primer sequences for *lacZ* determination have been described previously [27;28]. The experimental setup of the studies was examined and agreed upon by the institute's Ethical Committee on Experimental Animals, according to national legislation.

Experimental Design

Female mice were marked and randomized at the day of birth in different groups; i.e. longevity cohorts, or cross-sectional cohorts in which the mice were sacrificed at fixed time points. Cross-sectional cohorts of *Xpa*$^{-/-}$, *Xpc*$^{-/-}$ and their C57BL/6J controls were sacrificed at a fixed age of 13, 52, and 78 and 104 weeks. The interim cohorts consisted of at least 15 female mice per time point and genotype. In the longevity cohorts, a total of 45 *Xpa*$^{-/-}$ and 50 *Xpc*$^{-/-}$ female mice and 45 or 50 of their wild type controls (referred to in the text as C57BL/6J 1 and C57BL/6J 2) were monitored during their entire life span. The health state of the mice was checked daily, beginning at the day of weaning. Individual animals were weighed biweekly to determine live weights. During the entire experiment, animals were kept in the same stringently controlled (spf) environment, fed *ad libitum* and kept under a normal day/night rhythm. The microbiological status of the cohorts was monitored every 3 months. Animals from the longevity cohort were removed from the study when found dead or moribund. Complete autopsy was performed on animals of all cohorts; a total of 45 different tissues was isolated from each animal and stored for further histopathological analysis (see below). In addition, a selective set of 20 different tissues were snap frozen in liquid N_2 for molecular analyses, like *lacZ* mutant

frequency analyses. Total animal weights, as well as various organ weights, were determined at time of death or when killed.

Histopathology

Organ samples (45 organs and tissues) of each animal were preserved in a neutral aqueous phosphate-buffered 4% solution of formaldehyde. Tissues required for microscopic examination were processed, embedded in paraffin wax, sectioned at 5µm and stained with haematoxylin and eosin. Detailed microscopic examination was performed on 9 major organs of all female mice from the longevity cohort and on all gross lesions suspected of being tumors or representing major pathological conditions. For each animal, histopathological abnormalities, tumors as well as non-neoplastic lesions, were recorded using the PATHOS pathology data acquisition software and if possible, a cause of death was established.

Hprt *mutant frequency analyses*

Xpc$^{-/-}$, *Xpc*$^{+/-}$ mice and their wild type controls were sacrificed at 13 or 52 weeks and spleens were isolated to determine spontaneous *Hprt* mutant frequencies. All mice were in pure C57BL/6J background. The number of mice within one genotype and age group varied between 4 and 10.

Priming and cloning of T-lymphocytes was done in RPMI culture medium 1640 as described by Tates et al. [29] with some minor modifications [30]. Mouse T-lymphocytes were isolated from the spleen by rubbing the spleen through a sterile 70-µm nylon mesh (Falcon Cell Strainer, 2350). Subsequently cells were frozen in RPMI medium 1640 supplemented with 10% dimethyl sulfoxide and 40% fetal bovine serum by using a Cryomed freezing apparatus (Forma Scientific, Marietta, OH). When required, frozen cells were thawed and immediately stored on ice. Stimulated T-lymphocytes were cultured and selected for *Hprt*-deficiency in the presence of lethally irradiated (30 Gy X-rays) mouse lymphoblastoid Sp2/0 feeder cells [29]. Cloning efficiencies and mutant frequencies were calculated as described [29]. Further details on the procedure were described by Wijnhoven et al. [30].

LacZ *mutant frequency analyses*

From a selected set of snap frozen tissues DNA was extracted with a phenol/chloroform/iso-amyl alcohol mixture (25:24:1). Complete protocols for plasmid rescue and mutant frequency determinations with the pUR288 model have been described elsewhere [31]. Briefly, between 10 and 20 µg genomic DNA was digested with HindIII for 1 h in the presence of magnetic beads (Dynal), recoated with lacI–lacZ fusion protein. The beads were washed three times to remove the unbound mouse genomic DNA. Plasmid DNA was subsequently eluted from the beads by IPTG and circularized with T4 DNA ligase. Next, ethanol-precipitated plasmids were used to transform *E. coli C* (ΔlacZ, galE−) cells. One thousandth of the transformed cells was plated on the titer plate (with X-gal) and the remainder on the selective plate (with p-gal). The plates were incubated for 15 h at 37 ^{o}C. Mutant frequencies were determined as the number of colonies on the selective plates versus the number of colonies on the titer plate (times the dilution factor of 1000). Each mutant frequency is based on at least 300,000 recovered plasmids.

Statistical evaluation

Incidences of tumors were analyzed with the method of Peto (SAS) [32] and with the poly-3 and poly-k method [33]. These tests for statistical analysis of tumor incidences take differences in survival of the various groups into account. The poly-3 and poly-k test were performed by Dr H. Moon, California State University, Long Beach CA, USA.

Cell culture

Primary mouse embryonic fibroblasts (MEFs) were isolated from E13.5 day embryos, all in C57BL/6J background, and genotyped as described previously [27;28]. MEFs were cultured as described before [34] in Dulbecco's modified Eagle Medium (DMEM, Gibco) supplemented with 10% fetal bovine serum (FCS Biocell), 1% non essential amino acids (Gibco), penicillin (0,6 µg/ml) and streptomycin (1 µg/ml) at 37ºC, 5% CO_2. MEFs were cultured 3 days per passage at 3% or 20% O_2. Cell survival was determined by blue/white screening using Trypan Blue Stain 0.4% (Gibco) (1:1), counting a minimum of 200 cells per sample. A minimum of 3 different embryos were used per genotype, plus a technical replica of all samples was used.

Results

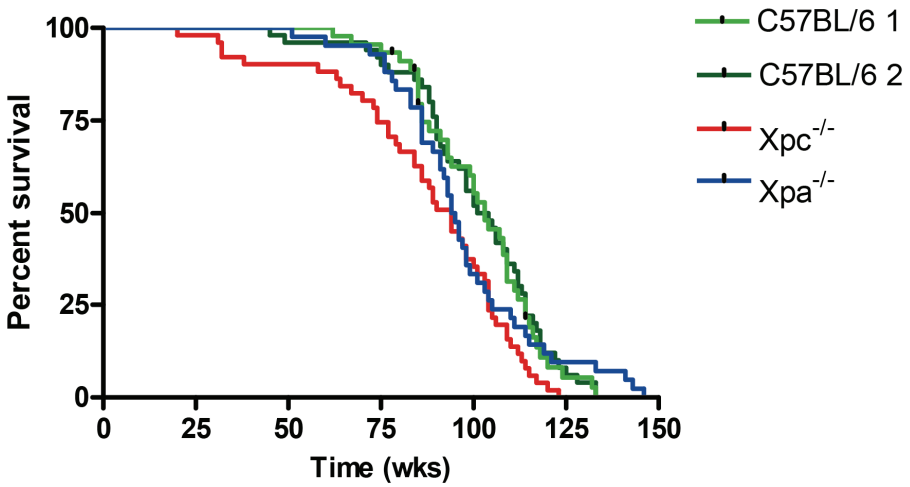

Figure 1. Survival curves of female *Xpc*$^{-/-}$, *Xpa-/-* and their wild type control cohorts. C57BL/6 1 is the control cohort for *Xpa*$^{-/-}$. C57BL/6 2 is the control cohort for *Xpc*$^{-/-}$. Median survival of the cohorts are: C57BL/6 1 = 103 weeks (light green line), C57BL/6 2 = 102.5 weeks (dark green line), *Xpc*$^{-/-}$ = 94 weeks (p = 0.0023) (red line), *Xpa*$^{-/-}$ = 94.5 weeks (p = 0.6023) (blue line). For further details see materials and methods.

To determine the average life span of *Xpc*$^{-/-}$ and *Xpa*$^{-/-}$ mice, 45-50 mutant females and corresponding C57BL/6J control mice were followed during aging. The survival curves for the longevity cohorts of female *Xpc*$^{-/-}$, *Xpa*$^{-/-}$ and both matching wild type control groups are depicted in Figure 1. The median survival of female *Xpc*$^{-/-}$ mice (94 weeks) was significantly reduced (p=0.0023, Kaplan-Meier with Log

rank test) compared to the median survival of their female wild type C57BL/6J controls (C57BL/6J 2, 102.5 weeks). Female *Xpa*$^{-/-}$ median survival (94.5 weeks) on the other hand was not significantly reduced (p=0.6023, Kaplan-Meier with Log rank test) compared to the median survival of its female C57BL/6J controls (C57BL/6J 1, 103 weeks). This difference in significance is mainly caused by the fact that a certain fraction (± 10%) of the *Xpa*$^{-/-}$ animals survive extremely long (see Figure 1). Survival curves of both wild type control studies show a very similar median survival and shape of the curve.

		WT1	*Xpa*$^{-/-}$	P-value	WT2	*Xpc*$^{-/-}$	P-value
	Number of animals (absolute)	*40*	*31*		*29*	*38*	
All organs	Tumor bearing animals	**30** (75)	**21** (68)		**24** (83)	**23** (61)	
Liver	Hepatocellular tumor	**0** (0)	**3** (10)	0.0002	**2** (7)	**5** (13)	*
Lung	Bronchiolo-alveolar tumor	**0** (0)	**2** (6)		**1** (3)	**6** (16)	0.02
Pituitary	Pars distalis adenoma	**20** (50)	**8** (26)	*	**20** (70)	**9** (24)	0.01
All organs	Pituitary adenomas excluded	**18** (45)	**19** (61)	0.001	**21** (72)	**23** (61)	**

Table 1. Tumor incidences and *p*-values for difference between mutant and their concurrent wild type group. Absolute values are in bold, percentages are between brackets. Statistics: poly-k test (poly-3 test and Peto test generally gave similar significances, though exact *p*-value may differ).

* = approaches significance with poly-3 test only (p=0.08 for Xpc-/- liver and p=0.054 for Xpa-/- pituitary).

** = not reaching significance with poly-k test, but *p*-value for the Peto test = 0.05 (positive trend) in this case

Of all groups approximately 30 or more animals were histopathologically examined. Neoplasms and inflammation (mainly ulcerative dermatitis) are the most common cause of demise in all groups, ranging from 72% in wild type controls up to 87 % in *Xpc*$^{-/-}$ mice (data not shown). Occasionally more than one pathological condition might have contributed to death, in which case the most pronounced condition was taken as cause of demise. Incidences of major tumor types at the time of death are listed in Table 1. *Xpa*$^{-/-}$ and *Xpc*$^{-/-}$ mice lived shorter than their respective wild type controls. Accordingly, lower tumor incidences were expected in the mutant animals, since they had less time to develop tumors. Statistical methods that take differences in survival into account were therefore used in this case to evaluate the significance of differences in tumor incidences. Nevertheless, some tumor types were increased in either *Xpc*$^{-/-}$ or *Xpa*$^{-/-}$ mice. *Xpc*$^{-/-}$ mice show a significant increase (p = 0.02) in bronchio-alveolar lung tumors and near significant elevation (p = 0.054) in hepatocellular tumors. *Xpa*$^{-/-}$ mice solely show a significant increase (p < 0.01) in hepatocellular tumors when compared to their matching wild type control group. Furthermore, female *Xpc*$^{-/-}$ mice also show a significant increase in acidophilic macrophage pneumonia (p = 0.032, data not shown), which is not apparent in *Xpa*$^{-/-}$ mice.

The percentage of tumor bearing NER-deficient animals (all types together) is surprisingly lower than the corresponding NER-proficient control groups. In addition to the shorter lifespan, the strong and significant decrease in benign pituitary adenomas in both *Xpc*$^{-/-}$ and *Xpa*$^{-/-}$ mice is mostly responsible for this lower percentage in tumor bearing animals. The increase in number of tumor bearing animals (excluding the pituitary adenomas and taking into account the survival distribution) reaches

significance for *Xpa*$^{-/-}$ mice ($p < 0.01$) and approaches significance for *Xpc*$^{-/-}$ animals ($p = 0.05$) using the Peto test.

Although a variety of non-neoplastic changes was observed in the organs of mutant as well as wild type mice, there were no obvious genotype specific pathologies typical for *Xpc*$^{-/-}$ or *Xpa*$^{-/-}$ mice. The observed changes belonged to the normal background pathology of C57BL/6J mice and generally occurred to about the same degree in all groups. Since mutant animals died slightly earlier than wild type mice it may well be that these spontaneous aging lesions occurred slightly earlier in *Xpc*$^{-/-}$ and *Xpa*$^{-/-}$ mice than in wild type animals. However, this aspect was not explicitly investigated in this study.

Mutant frequency analyses

A comprehensive analysis of spontaneous *Hprt* mutant frequency was performed with *Xpc*$^{-/-}$, *Xpc*$^{+/-}$ and their wild type control mice in a pure C57BL/6J background (Figure 2). At the age of 52 weeks, *Hprt* mutant frequencies in wild type mice (MF= $0.9x10^{-6}$) were in the same range as previously reported [23]. At this age, mutant frequencies in *Xpc*$^{-/-}$ and *Xpc*$^{+/-}$ mice were elevated 15 and 3 fold, respectively, when compared to their age-matched wild type controls. In addition, *Xpc*$^{-/-}$ mice of 13 weeks old already exhibited a 5-fold increase in mutant frequency compared to the 52 weeks old wild type control animals.

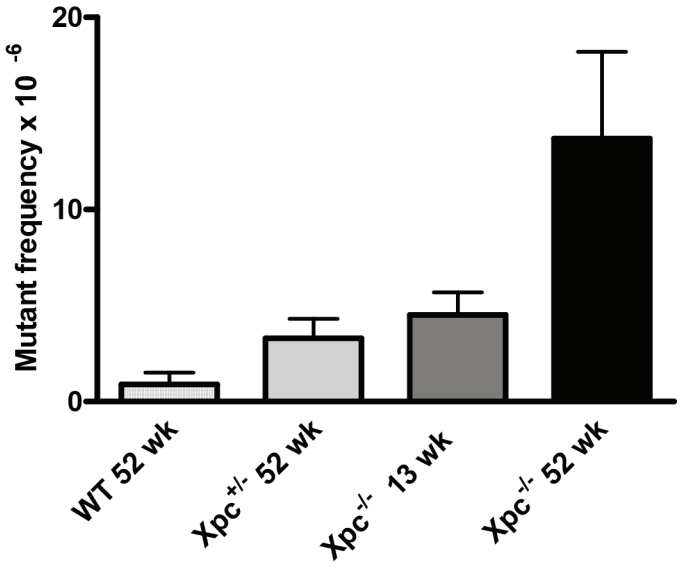

Figure 2. *Hprt* mutant frequencies including standard deviations of Xpc-/-, Xpc+/- and wild type controls at an age of 13 and 52 weeks in spleen. The numbers of biological replicas are between 4 and 10. For further details see Materials and Methods section.

In addition, we determined mutant frequencies in several tissues of C57BL/6J, *Xpc*$^{-/-}$ and *Xpa*$^{-/-}$ mice using the *LacZ* recovery system. Samples were taken from spleen, liver and lung of 13, 52 and 78 week old animals which were of age. Results are shown in Figure 3. Table 2 depicts the p-values of the

compared genotypes in all three tissues at different ages. Mutant frequencies increased over time in spleen, liver and lung of *Xpc*$^{-/-}$ mice. In *Xpa*$^{-/-}$ and C57BL/6J wild type mice an increase over time was visible in liver and lung, but not in spleen. Mutant frequencies in spleen showed a significant increase in mutants in 52 and 78 week old *Xpc*$^{-/-}$ mice compared to their age matched *Xpa*$^{-/-}$ and wild type samples (Figure 3A). Samples of *Xpa*$^{-/-}$ exhibited a similar *LacZ* mutant frequency pattern in the spleen as the wild type samples over the entire lifespan. The liver of *Xpc*$^{-/-}$ and *Xpa*$^{-/-}$ mice showed a strong increase in mutant frequency compared to that of wild type at 52 and 78 weeks of age (Figure 3B). *Xpc*$^{-/-}$ liver samples exhibited slightly higher values on average than *Xpa*$^{-/-}$ samples at those time points.

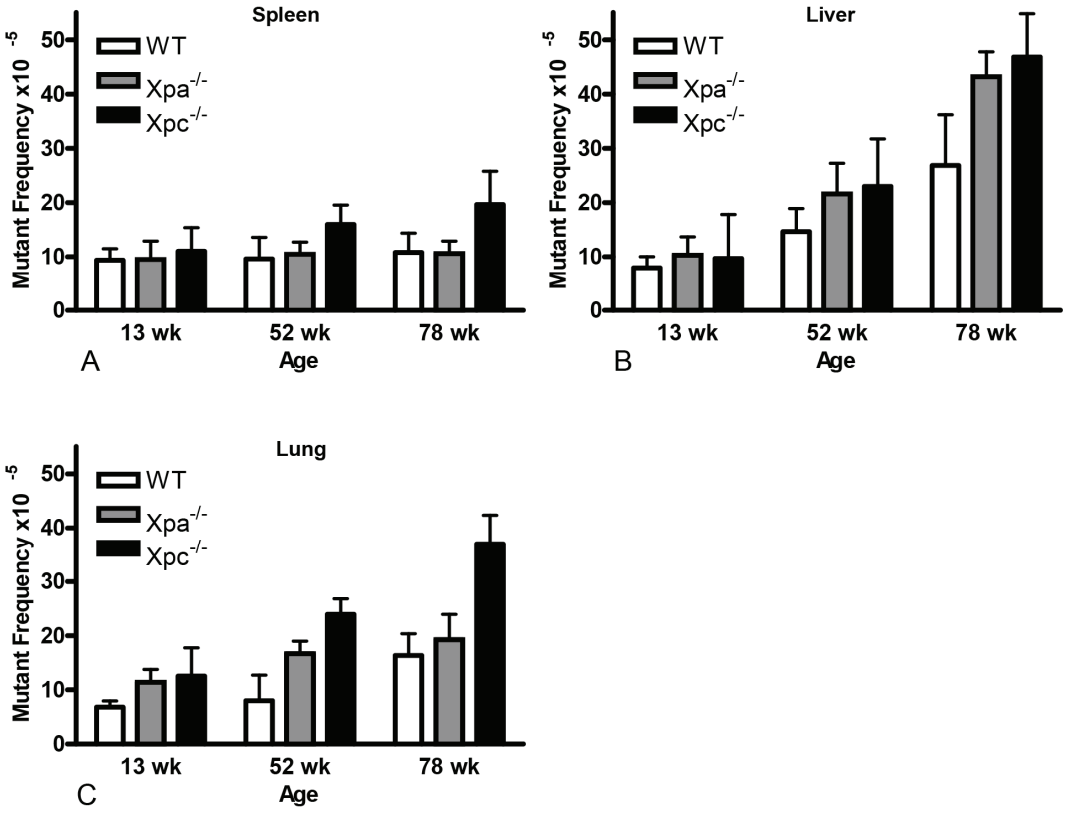

Figure 3. *LacZ* mutant frequencies including standard deviations of *Xpc*$^{-/-}$, *Xpa*$^{-/-}$ and wild type controls at an age of 13, 52 and 78 weeks in spleen (**A**), liver (**B**) and lung (**C**). The numbers of biological replicas are between 5 and 6. For further details see materials and methods.

The mutant frequency in *Xpc*$^{-/-}$ lung samples was significantly elevated in comparison to wild type controls at all time points. *Xpa*$^{-/-}$ mice only exhibited this increase at 13 and 52 week of age. At 78 weeks the mutant frequency of *Xpa*$^{-/-}$ lungs was comparable to that of wild type controls. Strikingly, *Xpc*$^{-/-}$ lungs showed a significant elevation in mutant frequency at an age of 52 and 78 weeks as compared to their NER-deficient counterpart *Xpa*$^{-/-}$. A twofold increase was visible in *Xpc*$^{-/-}$ lung samples at 78 weeks in relation to both wild type controls and *Xpa*-deficient samples (see Figure 3C).

Spleen	13wk	52wk	78wk	**Liver**	13wk	52wk	78wk	**Lung**	13wk	52wk	78wk
Xpc vs WT		*0.016*	*0.012*	***Xpc vs WT***			*0.002*	***Xpc vs WT***	*0.04*	*0.00003*	*0.0001*
Xpc vs Xpa		*0.0098*	*0.007*	***Xpc vs Xpa***				***Xpc vs Xpa***		*0.02*	*0.0005*
Xpa vs WT				***Xpa vs WT***		*0.04*	*0.002*	***Xpa vs WT***	*0.003*	*0.003*	

Table 2. *P*-values of mutant frequency comparisons between genotypes, depicted per age per tissue. Open cells represent non-significant ($p > 0.05$) differences.

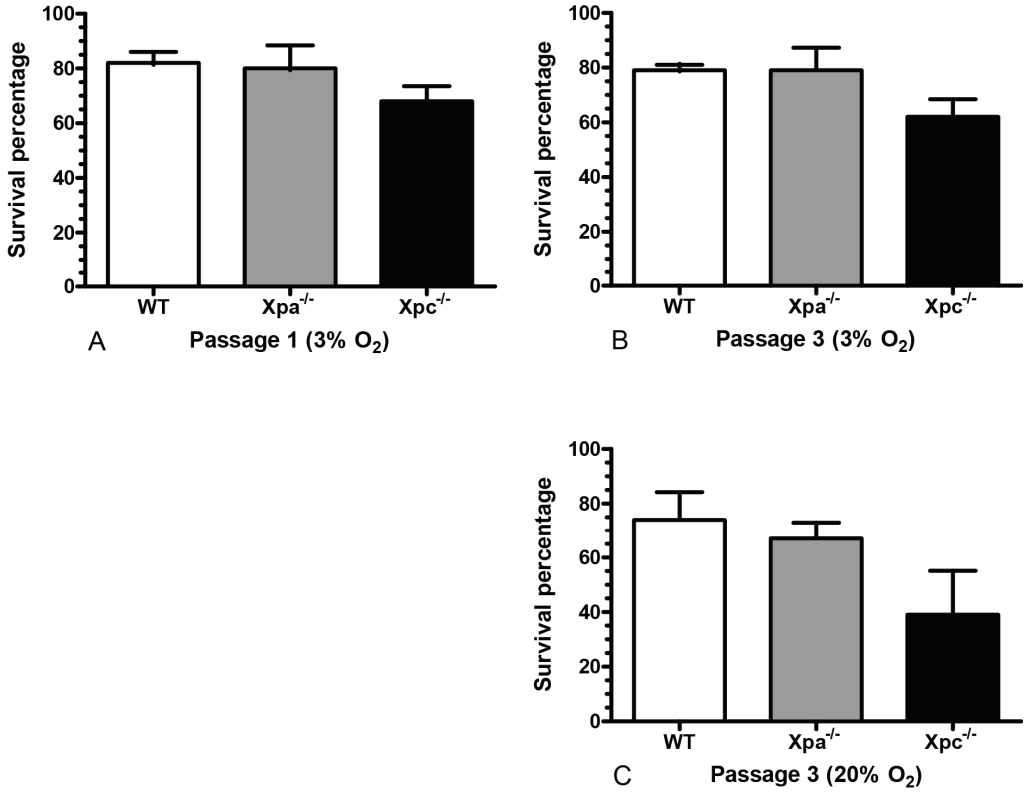

Figure 4. Survival of mouse embryonic fibroblasts including standard deviations of *Xpc*$^{-/-}$, *Xpa*$^{-/-}$ and their wild type controls under different levels of oxygen pressure. Cells at the first passage were all cultured at 3% oxygen (**A**); subsequent passages were cultured under 3% (**B**) or 20% oxygen (**C**), respectively.

Cell survival under oxygen exposure

In view of the increased tumor incidence and elevated spontaneous mutant frequency in lung we suspected that the *Xpc*$^{-/-}$ animals were more susceptible to oxidative stress. To directly test this hypothesis we investigated the effects of exposure to different levels of oxygen, 3% and 20%, on *Xpa*$^{-/-}$, *Xpc*$^{-/-}$ and wild type mouse embryonic fibroblasts (MEFs). Results are shown in Figure 4. *Xpc*$^{-/-}$ fibroblasts subjected to 3% oxygen level appeared to be slightly more sensitive than *Xpa*$^{-/-}$ and wild type MEFs in the first passage. Survival of *Xpc*$^{-/-}$ fibroblasts was 68% after 3 days of culturing (first passage in figure 4), while *Xpa*$^{-/-}$ and wild type fibroblasts exhibited 80% and 82% survival respectively. After two more passages, at 3% oxygen pressure, 62% survival was visible in cultured *Xpc*$^{-/-}$ fibroblasts that were cultured. The survival of *Xpa*$^{-/-}$ and wild type MEFs, at this point and under 3% oxygen pressure, was 79%. When, after the initial passage of 3% oxygen, the fibroblasts were cultured for two more passages at 20% oxygen pressure, a severe decrease in survival was exhibited in *Xpc*$^{-/-}$ fibroblasts. The percentage of survival dropped to a mere 39%. This dramatic decrease was not observed for *Xpa*$^{-/-}$ and wild type (67% and 74% survival respectively).

Discussion

Previous results obtained in separate studies in which patterns of survival, tumor formation and mutation accumulation were determined in *Xpc*- and *Xpa*-deficient mice were difficult to interpret because of variation in genetic background and the use of different mutational reporter genes. Here we performed a side-by-side comprehensive study of these endpoints in the same genetic background using both the *Hprt* and *LacZ* mutational target genes.

NER-deficient mouse models lacking a functional XPA or XPC protein show phenotypic differences when compared to their wild type controls. A significant reduction in spontaneous survival was observed in our comprehensive longevity studies for female *Xpc*-deficient mice in a pure C57BL/6J background. *Xpa*-deficient female mice also showed a decrease in survival when compared to their wild type control although not statistically significantly. Previously reported survival studies of *Xpc*$^{-/-}$ mice in a mixed background did not exhibit a decrease in survival [24]. Female *Xpa*$^{-/-}$ and *Xpc*$^{-/-}$ mice in our studies reached an average median age of 94.5 and 94 weeks, respectively, while their matching wild type controls attained a median survival of 103 and 102.5 weeks. Both the wild type control cohorts show a similar survival pattern and a comparable median age of 50% survival. As in humans, a deficiency in one of these NER proteins leads to a reduced lifespan and therefore XPA and XPC prove to be part of delicate and important processes that have a substantial effect on survival.

Additional pathological analyses of female *Xpa*$^{-/-}$ and *Xpc*$^{-/-}$ mice showed that the cause of death in many of these animals was not accountable to the presence of neoplasms. Another main cause of death of the NER-deficient mice was in fact the occurrence of inflammation, mainly ulcerative dermatitis. For the C57BL/6J 1 group (which was simultaneously executed with the *Xpa*$^{-/-}$ study) and *Xpa*$^{-/-}$ high incidences of inflammation were apparent (50 and 61% respectively). The C57BL/6J 2 and the *Xpc*$^{-/-}$ studies showed a somewhat lower incidence of inflammation (24% and 55% respectively). High incidences of ulcerative dermatitis in control C57BL/6J mice are considered an inevitable byproduct of handling the animals during their entire lifespan and are a result of a Staphylococcus aureus infection. Also the type of diet appears to play a role in the severity of this skin phenotype.

These findings are, however, clearly in line with our earlier findings [35] and those of others [36;37] working with particularly female C57BL/6J mice.

To our surprise the percentage of tumor bearing animals (TBA) was higher in NER-proficient mice than in the NER-deficient counterparts. This observation is, next to the longer lifespan observed in wild type mice, mostly attributable to a dramatic decrease in pituitary tumor development in *Xpc*$^{-/-}$ mice (from 70% to 24% occurrence) and in *Xpa*$^{-/-}$ mice (from 51% to 26% occurrence). A similar strong reduction in pituitary tumor development was observed in another NER-deficient mouse model, namely *Xpd*^{TTD} [35]. Here a significant decrease from 50% to 9% occurred. Interestingly, no such a decrease in pituitary tumor development was found in the TC-NER-deficient *Csb* mouse model (data not shown). Apparently, a defect in GG-NER is accompanied by suppression of a specific set of tumor types. Further studies are needed to substantiate this hypothesis.

A distinct difference between the two NER-deficient mouse models is the observed tumor spectrum. Female *Xpa*$^{-/-}$ mice exhibit a significant increase in hepatocellular adenomas compared to wild types. Female *Xpc*$^{-/-}$ mice also show an elevation in the number of hepatocellular neoplasms which approaches significance. Additionally, female *Xpc*$^{-/-}$ mice do show a significant increase in bronchio-alveolar neoplasms compared to their proficient controls. Such an increase is absent in female *Xpa*$^{-/-}$ mice.

Our results showed that female *Xpc*$^{-/-}$ mice in a pure C57BL/6J background are susceptible to lung cancer and support the previous findings of the lung cancer susceptibility in *Xpc*$^{-/-}$ mice in the more sensitive mixed background [24]. However, in this previous study the lung tumors observed and diagnosed as adenomas and adenocarcinomas appeared to be more malignant and were accompanied by a higher incidence of atypical hyperplasia. Possibly, depending on the genetic background and spontaneous (oxidative) DNA damage levels, tumors will progress earlier to a more malignant state. Next, several studies provide information that *Xpc* polymorphisms in humans may also contribute to genetic susceptibility for lung cancer [38-40]. Exposure of *Xpc*-deficient mice (in a mixed genetic background) to the harmful genotoxic carcinogen 2-AAF resulted in a significant elevation in the number of liver and lung tumors compared to wild type animals [18;41]. In contrast, *Xpa*$^{-/-}$ mice in a pure C57BL/6J background only show an elevation in liver tumors after exposure to 2-AAF and no increase in lung tumors was apparent in that study (18). The occurrence of lung tumors in *Xpc*$^{-/-}$ mice in pure C57BL/6J background after exposure to 2-AAF has not yet been assessed. The difference in tumor spectrum between *Xpc*$^{-/-}$ and *Xpa*$^{-/-}$ mice in our study indicates that the XPC protein is, besides active in NER, possibly also involved other repair systems, most likely including BER. This idea was recently also put forward by others [42]. The outcome of an increase in lung tumors in *Xpc*$^{-/-}$ mice could, therefore, point to an involvement of the XPC protein in the repair of oxidative DNA damage.

To analyze the mutation spectrum in DNA repair-deficient mice in the different organs, we conducted additional mutant frequency analyses on several tissues of wild type, *Xpa*$^{-/-}$ and *Xpc*$^{-/-}$ female mice. Initial spontaneous *Hprt* mutant analyses in spleen showed a strong increase of mutant frequency in T-lymphocytes of 52 week old *Xpc*$^{-/-}$ mice compared to their age-matched *Xpa*$^{-/-}$ and C57BL/6J controls. However, in an earlier study, *Xpc*$^{-/-}$ mice with a mixed background were used [23]. More comprehensive *Hprt* analyses using *Xpc*-deficient mice in a pure C57BL/6J background were performed here. The strong increase in mutant frequency compared to the wild type control was reproducible in *Xpc*$^{-/-}$ in a pure C57BL/6J background, albeit lower than in a mixed background. The results obtained with *LacZ*

mutant analyses show a more moderate response in spleen when *Xpc*$^{-/-}$ is compared to wild type. This can be explained by the fact that the background level of the *LacZ* mutant analyses is higher than that of *Hprt*. Although *Hprt* analysis is a more sensitive method than *LacZ* analyses, its drawback is that it is only applicable to the spleen. Other previous studies conducted here showed an elevation of mutant frequencies in *Xpa*$^{-/-}$ in liver and kidney using *LacZ* analyses [43;44].

Our results of the *LacZ* mutant analyses show a striking increase of mutant frequency in lung tissue of *Xpc*$^{-/-}$ mice when compared to wild type and *Xpa*$^{-/-}$ mice, especially at an age of 78 weeks. The fact that no severe increase in lung is observed in *Xpa*$^{-/-}$ mice but is distinctly present in *Xpc*$^{-/-}$ mice supports the hypothesis that the XPC protein might be involved in the removal of oxidative DNA damage since the level of oxidative stress is higher in lungs compared to other tissues due to the constant exposure of this tissue to oxygen [45]. In the spleen, *Xpc*$^{-/-}$ mice also shows a significant increase in mutant frequency compared to wild type and *Xpa*$^{-/-}$ at 52 and 78 weeks. In liver, on the other hand, the mutant frequencies of *Xpa*$^{-/-}$ and *Xpc*$^{-/-}$ liver are virtually equal over all time points. DNA damage in the liver most likely arises as a result of genotoxic bulky byproducts of metabolism. Compared to wild type, 78 week-old NER-deficient mouse livers do show a significant elevation of mutant frequency. This illustrates the sensitivity of the NER-deficient mouse strains to DNA damage. Over time and in all investigated tissues *Xpc*$^{-/-}$ mice show the highest mutant frequency, indicating an even higher sensitivity to DNA damage than *Xpa*$^{-/-}$ animals.

The putative role in the removal of oxidative damage is supported by our *in vitro* data, in which *Xpc*$^{-/-}$ mouse embryonic fibroblasts exhibit a severe decrease in survival when cultured at 20% oxygen compared to 3% oxygen pressure. We believe that the excess of oxidative damage is most likely the cause of death, since oxygen pressure is the only variable that was changed in culturing. *Xpc*-deficient fibroblasts seem to be impaired in the removal of this damage. Even at a low oxygen level of 3%, growth of *Xpc*-deficient cells seems more sensitive compared to *Xpa*-deficient and wild type fibroblasts.

The high mutant frequencies in oxygen rich surroundings in *Xpc*$^{-/-}$ cells and the severe decrease in cell survival under 20% oxygen pressure are concurrent with the present understandings and recent discoveries about the XPC protein. Several recent studies provide information about the involvement of XPC in base excision repair (BER) and the putative role in the repair of oxidative DNA damage. BER is mainly responsible for mending the DNA damage caused by oxidative stress [46]. XPC can physically and functionally interact with thymine DNA glycosylase, which plays a role in BER [47]. XPC-HR23B also has been assigned as a cofactor for base excision repair of 8-hydroxyguanine, by stimulating the activity of its specific DNA glycosylase OGG1 [48]. In addition, a recent study has shown a deficient BER after oxidative DNA damage induced by methylene blue plus visible light in XPC fibroblasts [49]. Methylene blue and visible light produce oxidative DNA damage, amongst others 8-OH-Gua.

Our results indicate the importance of the XPC protein in vivo, where the absence of the protein is responsible for susceptibility to lung tumors in mice compared to wild type and their NER-deficient counterpart *Xpa*$^{-/-}$. Mutant frequency analyses show an additional sensitivity in spleen compared to *Xpa*-deficient animals. In accordance with *Xpa*-deficiency, *Xpc*$^{-/-}$ mice also show a high mutant frequency in liver. Therefore our results, together with the accumulating evidence provided by others, support the theory of XPC involvement in BER or additional pathways and the removal of oxidative

DNA damage. A subsequent consequence of this engagement could explain the difference in tumor spectrum between *Xpa*$^{-/-}$ and *Xpc*$^{-/-}$ mice.

Acknowledgements

We are very grateful to Piet de With, Gwen Intres, Conny van Oostrom, Coen Moolenbeek, Christine Soputan, Sandra de Waal, Sisca de Vlugt and Ewoud Speksnijder for their skilful technical assistance. This work was financially supported by National Institute of Health (NIH)/National Institute of Aging (NIA), grant number 1 PO1 AG-17242, NIEHS (1UO1 ES011044), Netherlands Organization for Scientific Research (NWO) through the foundation of the Research Institute Diseases of the Elderly, as well as grants from the Dutch Cancer Society, (EUR 99-2004) and EC (QRTL-1999-02002).

Reference List

[1] C.Lengauer, K.W.Kinzler, B.Vogelstein. Genetic instabilities in human cancers, Nature, 396, (1998) 643-649.

[2] M.Takata, M.S.Sasaki, E.Sonoda, C.Morrison, M.Hashimoto, H.Utsumi, Y.Yamaguchi-Iwai, A.Shinohara, S.Takeda. Homologous recombination and non-homologous end-joining pathways of DNA double-strand break repair have overlapping roles in the maintenance of chromosomal integrity in vertebrate cells, EMBO J., 17, (1998) 5497-5508.

[3] E.C.Friedberg. DNA damage and repair, Nature, 421, (2003) 436-440.

[4] E.C.Friedberg. How nucleotide excision repair protects against cancer, Nat.Rev.Cancer, 1, (2001) 22-33.

[5] A.S.Balajee, V.A.Bohr. Genomic heterogeneity of nucleotide excision repair, Gene, 250, (2000) 15-30.

[6] B.S.Thoma, K.M.Vasquez. Critical DNA damage recognition functions of XPC-hHR23B and XPA-RPA in nucleotide excision repair, Mol.Carcinog., 38, (2003) 1-13.

[7] W.C.van der, J.Jansen, H.Vrieling, L.A.van der, A.Van Zeeland, L.Mullenders. Nucleotide excision repair in differentiated cells, Mutat.Res., 614, (2007) 16-23.

[8] K.H.Kraemer, N.J.Patronas, R.Schiffmann, B.P.Brooks, D.Tamura, J.J.DiGiovanna. Xeroderma pigmentosum, trichothiodystrophy and Cockayne syndrome: a complex genotype-phenotype relationship, Neuroscience, 145, (2007) 1388-1396.

[9] J.de Boer, J.H.Hoeijmakers. Nucleotide excision repair and human syndromes, Carcinogenesis, 21, (2000) 453-460.

[10] D.Bootsma, G.Weeda, W.Vermeulen, H.van Vuuren, C.Troelstra, S.P.van der, J.Hoeijmakers. Nucleotide excision repair syndromes: molecular basis and clinical symptoms, Philos.Trans.R.Soc.Lond B Biol.Sci., 347, (1995) 75-81.

[11] T.Yasuda, K.Sugasawa, Y.Shimizu, S.Iwai, T.Shiomi, F.Hanaoka. Nucleosomal structure of undamaged DNA regions suppresses the non-specific DNA binding of the XPC complex, DNA Repair (Amst), 4, (2005) 389-395.

[12] P.C.Hanawalt, J.M.Ford, D.R.Lloyd. Functional characterization of global genomic DNA repair and its implications for cancer, Mutat.Res., 544, (2003) 107-114.

[13] M.Yokoi, C.Masutani, T.Maekawa, K.Sugasawa, Y.Ohkuma, F.Hanaoka. The xeroderma pigmentosum group C protein complex XPC-HR23B plays an important role in the recruitment of transcription factor IIH to damaged DNA, J.Biol.Chem., 275, (2000) 9870-9875.

[14] K.Sugasawa. The xeroderma pigmentosum group C protein complex and ultraviolet-damaged DNA-binding protein: functional assays for damage recognition factors involved in global genome Repair, Methods Enzymol., 408, (2006) 171-188.

[15] C.J.Park, B.S.Choi. The protein shuffle. Sequential interactions among components of the human nucleotide excision repair pathway, FEBS J., 273, (2006) 1600-1608.

[16] R.M.Costa, V.Chigancas, R.S.Galhardo, H.Carvalho, C.F.Menck. The eukaryotic nucleotide excision repair pathway, Biochimie, 85, (2003) 1083-1099.

[17] J.E.Cleaver. Cancer in xeroderma pigmentosum and related disorders of DNA repair, Nat.Rev.Cancer, 5, (2005) 564-573.

[18] E.M.Hoogervorst, C.T.van Oostrom, R.B.Beems, J.van Benthem, B.J.van den, C.F.van Kreijl, J.G.Vos, A.de Vries, H.van Steeg. 2-AAF-induced tumor development in nucleotide excision repair-deficient mice is associated with a defect in global genome repair but not with transcription coupled repair, DNA Repair (Amst), 4, (2005) 3-9.

[19] A.de Vries, C.T.van Oostrom, F.M.Hofhuis, P.M.Dortant, R.J.Berg, F.R.de Gruijl, P.W.Wester, C.F.van Kreijl, P.J.Capel, H.van Steeg, . Increased susceptibility to ultraviolet-B and carcinogens of mice lacking the DNA excision repair gene XPA, Nature, 377, (1995) 169-173.

[20] G.T.van der Horst, H.van Steeg, R.J.Berg, A.J.van Gool, J.de Wit, G.Weeda, H.Morreau, R.B.Beems, C.F.van Kreijl, F.R.de Gruijl, D.Bootsma, J.H.Hoeijmakers. Defective transcription-coupled repair in Cockayne syndrome B mice is associated with skin cancer predisposition, Cell, 89, (1997) 425-435.

[21] R.J.Berg, A.de Vries, H.van Steeg, F.R.de Gruijl. Relative susceptibilities of XPA knockout mice and their heterozygous and wild-type littermates to UVB-induced skin cancer, Cancer Res., 57, (1997) 581-584.

[22] L.B.Meira, A.M.Reis, D.L.Cheo, D.Nahari, D.K.Burns, E.C.Friedberg. Cancer predisposition in mutant mice defective in multiple genetic pathways: uncovering important genetic interactions, Mutat.Res., 477, (2001) 51-58.

[23] S.W.Wijnhoven, H.J.Kool, L.H.Mullenders, A.A.van Zeeland, E.C.Friedberg, G.T.van der Horst, H.van Steeg, H.Vrieling. Age-dependent spontaneous mutagenesis in Xpc mice defective in nucleotide excision repair, Oncogene, 19, (2000) 5034-5037.

[24] M.C.Hollander, R.T.Philburn, A.D.Patterson, S.Velasco-Miguel, E.C.Friedberg, R.I.Linnoila, A.J.Fornace, Jr. Deletion of XPC leads to lung tumors in mice and is associated with early events in human lung carcinogenesis, Proc.Natl.Acad.Sci.U.S.A, 102, (2005) 13200-13205.

[25] A.de Vries, H.van Steeg. Xpa knockout mice, Semin.Cancer Biol., 7, (1996) 229-240.

[26] D.L.Cheo, H.J.Ruven, L.B.Meira, R.E.Hammer, D.K.Burns, N.J.Tappe, A.A.van Zeeland, L.H.Mullenders, E.C.Friedberg. Characterization of defective nucleotide excision repair in XPC mutant mice, Mutat.Res., 374, (1997) 1-9.

[27] M.E.Dolle, H.Giese, C.L.Hopkins, H.J.Martus, J.M.Hausdorff, J.Vijg. Rapid accumulation of genome rearrangements in liver but not in brain of old mice, Nat.Genet., 17, (1997) 431-434.

[28] S.W.Wijnhoven, H.J.Kool, L.H.Mullenders, R.Slater, A.A.van Zeeland, H.Vrieling. DMBA-induced toxic and mutagenic responses vary dramatically between NER-deficient Xpa, Xpc and Csb mice, Carcinogenesis, 22, (2001) 1099-1106.

[29] A.D.Tates, F.J.van Dam, A.T.Natarajan, A.H.Zwinderman, S.Osanto. Frequencies of HPRT mutants and micronuclei in lymphocytes of cancer patients under chemotherapy: a prospective study, Mutat.Res., 307, (1994) 293-306.

[30] S.W.Wijnhoven, E.Sonneveld, H.J.Kool, C.M.van Teijlingen, H.Vrieling. Chemical carcinogens induce varying patterns of LOH in mouse T-lymphocytes, Carcinogenesis, 24, (2003) 139-144.

[31] M.E.Dolle, H.J.Martus, J.A.Gossen, M.E.Boerrigter, J.Vijg. Evaluation of a plasmid-based transgenic mouse model for detecting in vivo mutations, Mutagenesis, 11, (1996) 111-118.

[32] R.Peto, M.C.Pike, N.E.Day, R.G.Gray, P.N.Lee, S.Parish, J.Peto, S.Richards, J.Wahrendorf. Guidelines for simple, sensitive significance tests for carcinogenic effects in long-term animal experiments, IARC Monogr Eval.Carcinog.Risk Chem.Hum.Suppl, (1980) 311-426.

[33] H.Moon, H.Ahn, R.L.Kodell. An age-adjusted bootstrap-based Poly-k test, Stat.Med., 24, (2005) 1233-1244.

[34] J.Brugarolas, C.Chandrasekaran, J.I.Gordon, D.Beach, T.Jacks, G.J.Hannon. Radiation-induced cell cycle arrest compromised by p21 deficiency, Nature, 377, (1995) 552-557.

[35] S.W.Wijnhoven, R.B.Beems, M.Roodbergen, B.J.van den, P.H.Lohman, K.Diderich, G.T.van der Horst, J.Vijg, J.H.Hoeijmakers, H.van Steeg. Accelerated aging pathology in ad libitum fed Xpd(TTD) mice is accompanied by features suggestive of caloric restriction, DNA Repair (Amst), 4, (2005) 1314-1324.

[36] R.J.Kastenmayer, M.A.Fain, K.A.Perdue. A retrospective study of idiopathic ulcerative dermatitis in mice with a C57BL/6 background, J.Am.Assoc.Lab Anim Sci., 45, (2006) 8-12.

[37] G.W.Lawson, A.Sato, L.A.Fairbanks, P.T.Lawson. Vitamin E as a treatment for ulcerative dermatitis in C57BL/6 mice and strains with a C57BL/6 background, Contemp.Top.Lab Anim Sci., 44, (2005) 18-21.

[38] G.Y.Lee, J.S.Jang, S.Y.Lee, H.S.Jeon, K.M.Kim, J.E.Choi, J.M.Park, M.H.Chae, W.K.Lee, S.Kam, I.S.Kim, J.T.Lee, T.H.Jung, J.Y.Park. XPC polymorphisms and lung cancer risk, Int.J.Cancer, 115, (2005) 807-813.

[39] Y.Bai, L.Xu, X.Yang, Z.Hu, J.Yuan, F.Wang, M.Shao, W.Yuan, J.Qian, H.Ma, Y.Wang, H.Liu, W.Chen, L.Yang, G.Jing, X.Huo, F.Chen, Y.Liu, L.Jin, Q.Wei, W.Huang, H.Shen, D.Lu, T.Wu. Sequence variations in DNA repair gene XPC is associated with lung cancer risk in a Chinese population: a case-control study, BMC.Cancer, 7, (2007) 81.

[40] Z.Hu, Y.Wang, X.Wang, G.Liang, X.Miao, Y.Xu, W.Tan, Q.Wei, D.Lin, H.Shen. DNA repair gene XPC genotypes/haplotypes and risk of lung cancer in a Chinese population, Int.J.Cancer, 115, (2005) 478-483.

[41] D.L.Cheo, D.K.Burns, L.B.Meira, J.F.Houle, E.C.Friedberg. Mutational inactivation of the xeroderma pigmentosum group C gene confers predisposition to 2-acetylaminofluorene-induced liver and lung cancer and to spontaneous testicular cancer in Trp53-/- mice, Cancer Res., 59, (1999) 771-775.

[42] D.Nahari, L.D.McDaniel, L.B.Task, R.L.Daniel, S.Velasco-Miguel, E.C.Friedberg. Mutations in the Trp53 gene of UV-irradiated Xpc mutant mice suggest a novel Xpc-dependent DNA repair process, DNA Repair (Amst), 3, (2004) 379-386.

[43] M.E.Dolle, R.A.Busuttil, A.M.Garcia, S.Wijnhoven, E.van Drunen, L.J.Niedernhofer, H.G.van der, J.H.Hoeijmakers, H.van Steeg, J.Vijg. Increased genomic instability is not a prerequisite for shortened lifespan in DNA repair deficient mice, Mutat.Res., 596, (2006) 22-35.

[44] H.Giese, M.E.Dolle, A.Hezel, H.van Steeg, J.Vijg. Accelerated accumulation of somatic mutations in mice deficient in the nucleotide excision repair gene XPA, Oncogene, 18, (1999) 1257-1260.

[45] d.van, V, C.E.Cross. Oxidants, nitrosants, and the lung, Am.J.Med., 109, (2000) 398-421.

[46] T.K.Hazra, A.Das, S.Das, S.Choudhury, Y.W.Kow, R.Roy. Oxidative DNA damage repair in mammalian cells: a new perspective, DNA Repair (Amst), 6, (2007) 470-480.

[47] Y.Shimizu, S.Iwai, F.Hanaoka, K.Sugasawa. Xeroderma pigmentosum group C protein interacts physically and functionally with thymine DNA glycosylase, EMBO J., 22, (2003) 164-173.

[48] M.D'Errico, E.Parlanti, M.Teson, B.M.de Jesus, P.Degan, A.Calcagnile, P.Jaruga, M.Bjoras, M.Crescenzi, A.M.Pedrini, J.M.Egly, G.Zambruno, M.Stefanini, M.Dizdaroglu, E.Dogliotti. New functions of XPC in the protection of human skin cells from oxidative damage, EMBO J., (2006).

[49] S.N.Kassam, A.J.Rainbow. Deficient base excision repair of oxidative DNA damage induced by methylene blue plus visible light in xeroderma pigmentosum group C fibroblasts, Biochem.Biophys.Res.Commun., 359, (2007) 1004-1009.